International Research Journal of Engineering and Technology (IRJET) e-ISSN: 2395-0056
Volume: 13 Issue: 06 | Jun 2026 www.irjet.net p-ISSN: 2395-0072

ROOT BENDING STRESS IN CYLINDRICAL WORM GEARS

[1]Edward E. Osakue, [2]Boma Afiesimama

[12]Department of Aerospace and Mechanical Engineering, Texas Southern University, Houston, Texas, USA

ABSTRACT-*A model for estimating the root bending stress of cylindrical worm gears, which are special types of cylindrical helical gears, is presented. The formulation of the model started with the root bending stress formula for cylindrical helical gears that was modified by making adjustments for some of the unique features of worm gears. Based on the geometry of a throated worm gear, some stress modification factors were defined, estimated and applied to the stress model of cylindrical helical gears. The outcome is a new cylindrical worm root bending stress model which suggests that worm gears potentially have 34% higher root bending stress capacity than equivalent cylindrical helical gears. The gain in strength is largely due to the throating of the worm gear. The bending stress model is used to estimate the root bending stress of five wormsets from references of varied backgrounds, and the results are compared with the previous solutions. The variances between stresses from the current and previous solutions when all basic design parameters are matched are in the range of -32.3 to -3.8% indicating that the previous solutions seem conservative relative to the new model solutions. This is not unexpected since the models in the references do not incorporate all the design parameters of a wormset as the new model. When the new model approach is used without matching the estimated service load factors with the values in the references, the variances between the current and previous results are between -13.3% and 2.4%, which seems very reasonable. Considering the diverseness of the sources of the references, such variances seem remarkable. Hence, the new root bending stress model appears sufficiently accurate to be an attractive option in the design analysis of cylindrical worm gears.*

Keywords: mesh, contact ratio, throating, load sharing, bending stress, failure, yielding, fracture

1.0 INTRODUCTION

Worm gears mate with worm threads in wormsets to form gear drives that are compact and give high transmission ratios. The popular types of wormsets are cylindrical and globoidal wormsets and the less common types are straight and spiroid wormsets. A cylindrical wormset is shown in Fig. 1a and has a gear throated in the axial plane, but the worm is not throated. Fig. 1b shows a globoidal wormset which has both the gear and worm throated. This study is focused only on cylindrical worm gears.

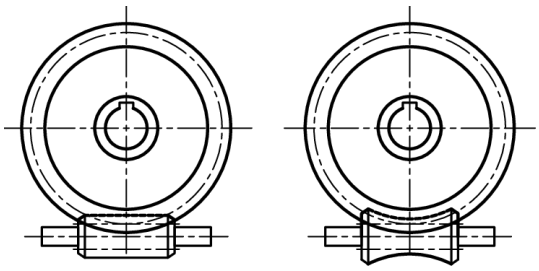

a) Cylindrical b) Globoidal

Fig. 1: Common wormsets

The function of a gear drive is to reliably transmit power and or motion at acceptable levels of noise, vibration, and temperature [1] with adequate service life. The service life of gears depends principally on the contact stress and the root bending stress levels in operation. This study is concerned with the root bending stress capacity of cylindrical wormsets. Generally, higher root bending stresses have greater probability of early gear failure which often occurs at the gear root where the bending stress is a maximum. Cracks are initiated in the root region of gear teeth when the operating bending stress exceeds the strength capacity of the gear material. Cracks usually grow with time and may lead to fracture of the gear tooth. Gear tooth breakage can be caused by sustained fatigue load of low to medium values at high number of load cycles as in normal fatigue, high load with low number of cycles or by a single severe momentary overload [1]. Momentary gear overload occurs during startup, breaking or shutdown [2]. At high torque and low speed, the root bending capacity of worm gears is the dominant design criterion [3]. Also, bending stress failure in worm gears can become an issue when the number of gear teeth is high, like 100 teeth and above [2].

Some gear design standards estimate the bending strength capacity of worm gear teeth using the nominal root shear stress. Though, this method provides an easy solution, it is only well suited to small center distances of about 100 mm [4]. The method tends to underestimate the actual service life of worm gears, because the stress estimates are likely conservative. The von Mises stress which combines the

shear and bending stresses at the gear root is used by some design standards. This method tends to give some improvement for a wider variety of worm gears [4]. The intricate form of the worm gear tooth due to varying cross-section along its length and its curved section make it extremely difficult to accurately determine the bending stress in worm gears [5]. Hence, the root bending capacity of worm gears is not well known [4]. This study was conducted with the objective of formulating a more analytical and scientific model for the bending stress capacity of cylindrical worm gears. Specifically, it was to develop a root bending stress model that will allow a worm gear to be treated as a cylindrical helical gear in bending stress analysis. Presumably, this would provide a more rational approach and reliable basis for the design analysis of the root bending stress in cylindrical wormsets.

2.0 WORM THREAD AND WORM GEAR PROFILES

A worm may be considered as a helical rack, but it is practically a special type of power screw. The thread profile of a worm may be trapezoidal, involute or some other profile [2]. The common worm thread profiles are designated as ZA, ZN, ZK, ZI, and ZC [6]. The ZA has a trapezoidal or Archimedean section with straight sides in the axial plane. Archimedean gearing resembles a linear rack and helical gearset. The ZN has a trapezoidal section with straight sides in the normal plane but a prolate involute in the transverse plane. The ZK has a convex profile in the normal plane and concave profile in axial section. The ZI has an involute profile in the axial plane like a helical gear. A special worm with concave profile in the axial section is CAVEX or ZC. It offers better contact conditions and higher load capacity.

In common practice, straight cylindrical worms with trapezoidal profile of 40^o included angle and gear of involute profile are used in wormsets [2, 6, 7]. The most popular worm type is the Archimedean worm that has straight-sided threads in its axial plane of the worm. The number of threads on a worm may be from 1 to 10 [8, 9], but more threads may be used in large units. However, 1 to 6 threads are popular in power transmission drives, with even number threads preferred to odd [10]. Higher number of threads is associated with lower speed ratios and gives higher mesh efficiency. At higher center distances, the worm pitch diameter becomes large, and more threads are required to improve efficiency. A worm can be made integral with a shaft or as a shell that is mounted on the shaft with splines, keys, or pins depending on the load capacity.

A worm gear is a specially modified helical gear with a helix angle equal to the lead angle of the worm and has the same hand as the worm thread. The worm gear tooth profile is often that of an involute which is a standard tooth profile. In the diametral plane of a cylindrical worm gear, the engagement between the gear and a worm is similar to that of a helical gear and a rack. The axial pitch of the worm thread is equal to the circular pitch of the gear. In wormsets. the axial plane of the gear corresponds to diametral plane of the worm and verse versa. However, the pair shares a common normal section, which may be used for defining wormset profiles by specifying the normal module as standard module. The modifications in worm gear profile include but not limited to throating and tooth thickness. Throating allows the gear to partially wrap around the worm, or vice versa, thereby enhancing greater contact between the pairs with increased load capacity. It also reduces the bending moment at the root of the gear by preventing the concentration of load on the tip region of the gear profile. The backlash in cylindrical worm gears is applied on the worm threads, making the tooth thickness of worm gears very slightly more than that of cylindrical helical gears. Other peculiarities of worm gears are discussed later.

3.0 SPUR GEAR EQUIVALENCE OF HELICAL GEAR

A spur gear basically has two planes associated with it, which are the transverse and axial planes. The transverse plane is the plane of rotation and is perpendicular to the axial plane. The gear diameter is defined on the transverse plane, while the gear facewidth is defined on the axial plane. Helical gears have a normal plane, where the tooth profile is defined, in addition to the axial and transverse planes of spur gears. In a spur gear, the normal and transverse planes are coincident. Like spur gears, the driving force in helical gears lies in the transverse plane but actual contact of gear teeth occurs in the normal plane. The shape of a helical gear in the normal plane is almost exactly the same as that of a spur gear with a larger number of teeth [11]. Hence an equivalent spur for a helical may be defined on the normal plane. The equivalent spur gear is assumed to have a tooth profile identical to the tooth profile of a gear on the normal plane [12] and has the same load capacity as the helical gear. The two parameters which relate a helical to its equivalent spur gear are the transverse pressure angle and the base helix angle [13]. When the normal pressure angle is standardized for helical gears, then:

$$\phi_t = \tan^{-1}\left[\frac{\tan\phi_n}{\cos\psi}\right] \qquad \psi_b = \tan^{-1}\left[\tan\psi\cos\phi_t\right] \qquad (1)$$

Note that Eq. (1) has two expressions which should be interpreted as Eq. (1a) and Eq. (1b) from left to right. All other equations below with more than one expression should be similarly interpreted. Please, refer to the

Nomenclature for the definition of parameters in the equation and others that follow.

According to Maitra [6], the base helix angle (Eq. (1b)), gives a more accurate estimate of the radius of curvature of an equivalent spur gear on the plane of contact. Consequently, it may be used to define a virtual plane for a helical gear where an equivalent or virtual spur gear may the analyzed. When the worm is considered as a helical rack in a wormset, it is associated with an infinite radius of curvature because it's profile in the plane of engagement with a gear has straight flanks. Therefore, the virtual number of teeth for the worm is given by Eq. (2a). The virtual number of teeth for the worm gear is given by Eq. (2b).

$$z_{v1} = \infty \qquad z_{v2} \approx \frac{z_2}{\cos^3 \psi_b} \qquad (2)$$

The speed ratio of a wormset and optimum lead angle are given in Eq. (3a) and Eq. (3b), respectively.

$$u = \frac{N_1}{N_2} \qquad \gamma_o = \tan^{-1}\left(\frac{1}{u}\right)^{1/3} \qquad (3)$$

The minimum number of teeth for worm gears of 20° standard pressure angle is between 21 and 29 [2, 5, 11] with an average of 25. Often a choice of the number of threads on a worm is necessary and the number may be chosen using Eq, (4a) as a guide. The next higher integer may be chosen for improved efficiency of the drive, the default is the lower integer number. The number of gear teeth is obtained from Eq. (4b)

$$z_1 \approx \frac{1}{2}\left[\frac{25}{u} + \frac{\gamma_o}{6}\right] \qquad z_2 = z_1 u \qquad (4)$$

The number of worm threads and gear teeth may be selected to get a hunting tooth for multiple threaded worms. A hunting tooth on the gear helps to distribute wear more evenly amongst gear teeth. This can be achieved by ensuring that the speed ratio is not an integer when multiple threaded worms are used.

4.0 WORMSET LOADS

Fig. 2 shows the forces acting in a worm drive. The forces are assumed to act on the pitch diameters of the worm and gear and the input is at the worm which is the most common configuration. The frictional force in the contact zone of wormsets cannot be neglected as in other types of gears because of the higher sliding velocity in the mesh. Considerable heat is generated in the mesh due to friction which makes scoring wear failure common in wormsets. It is, therefore, important to minimize friction in the mesh for adequate service life.

The power transmitted by wormsets gives rise to loads like torques and forces on the gear and worm that are transmitted to the supporting shafts, bearings, and housings. The input and output powers are related as:

$$P_2 = \eta_w P_1 \qquad (5)$$

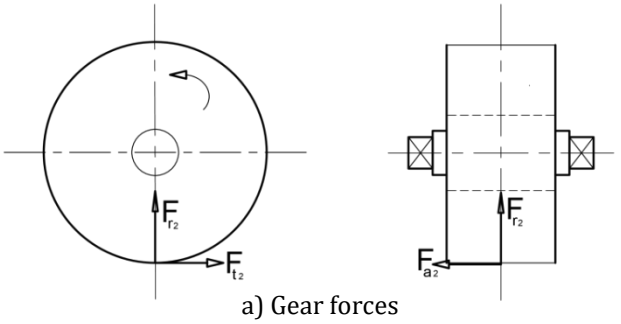

a) Gear forces

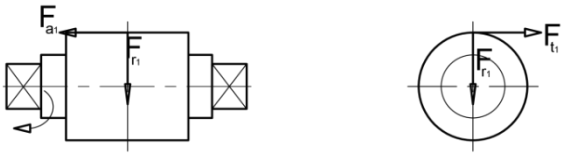

b) Worm forces

Fig. 2: Forces in worm drives

The torque loads in the drive are:

$$T_2 = \frac{\eta_w P_1 \times 10^3}{\pi N_2} \qquad T_2 = u \eta_w T_1 \qquad (6)$$

Fig 2a shows the forces on the gear while Fig. 2b shows those on the worm. The normal contact force is assumed to act at the pitch point. The tangential forces are obtained from Eq. (7).

$$F_{t1} = \frac{2T_1 \times 10^3}{d_1} = -F_{a2} \qquad F_{t2} = \frac{2T_2 \times 10^3}{d_2} = -F_{a1} \qquad (7)$$

The radial and normal forces are given by Eq. (8a) and Eq. (8b), respectively.

$$F_{r2} = F_{t2} \tan \phi_t = -F_{r1} \qquad F_n = \frac{k_c F_t}{\cos \phi_n \cos \psi} \qquad (8)$$

The friction force coefficient and axial force factor are given by Eq. (9a) and Eq. (9b), respectively.

Most gears, including wormsets are under sustained fatigue loading in operation. A component under fatigue load may experience one (uni) directional or two (bi) directional loading. The direction of the load is fixed in only one direction in unidirectional loading, but in bidirectional loading there is a partial or complete reversal of the load direction. Components that are loaded in one direction are said to be in pulsating fatigue and those loaded in both directions are said to be in fully reversed or alternating fatigue. If a wormset is self-locking, the gear is unable to drive the worm, that is, only the worm can drive the gear, and the worm gear is subjected to pulsating load. Self-locking may occur at low lead angles less than 6° [14] If the worm gear is designed to drive the worm, the wormset is described as "back-driving" or overhauling. In this case, the worm gear is loaded in both directions and under fully reversed fatigue loading. Back-driving may occur at lead angles greater than 10° [14]. Gears under fully reversed fatigue loading are more prone to fatigue failure than those under pulsating load.

5.0 SERVICE LOAD FACTOR (K_s)

Experience shows that the forces acting on devices in service are generally higher than the rated or nominal values in gear drives. Practically, the design or service load is often estimated by multiplying the rated load with a service load factor. This is used to account for load increases during normal operations of gearsets, but not for occasional overloads. The service load factor may be evaluated as indicated in Eq. (10) [13, 15].

$$K_s = K_a K_v K_m K_f K_w \tag{10}$$

Methods for evaluating K_v , K_m and K_r can be found in [13, 15, 16] and AGMA documents [17]. AGMA [17] gives recommendations on the selection of K_a . Please, refer to Appendix A for a summary of a method for estimating K_s .

6.0 BENDING RESISTANCE OF HELICAL GEAR

A gear tooth in a mesh acts like a cantilever beam as it resists the forces transmitted during operation. Fig. 3 shows a spur gear tooth with the transmitted tangential and radial forces applied at the tip as modeled by Lewis [13]. During meshing, the contact point of the load changes from the tip or addendum radius to the clearance circle radius. The tangential component of force induces both bending and shear stresses at the gear root. The radial component of force causes only compressive stress at the gear root and the bending moment from the radial force component is

$$k_c = \left[1 - \frac{\vartheta_m \tan\psi}{\cos\phi_n}\right]^{-1} \qquad \chi_a = \frac{F_a}{F_t} \tag{9}$$

assumed negligible. The highest tensile bending stress occurs near the gear root on the loaded side of the tooth [18]. A fillet is usually provided at the gear tooth root area to connect the gear tooth profile to the root or dedendum circle of the gear tooth. The discontinuity caused by the fillet creates some stress concentration, making it the critical point in fatigue failure consideration. Fatigue failures are often caused by tensile stresses since compressive stresses tend to enhance fatigue resistance [19]. A crack normally initiates at a discontinuity where there is a cyclic maximum tensile stress. Cracks grow along planes normal to the maximum tensile stress and when the growth becomes unstable, brittle fracture rapidly follows.

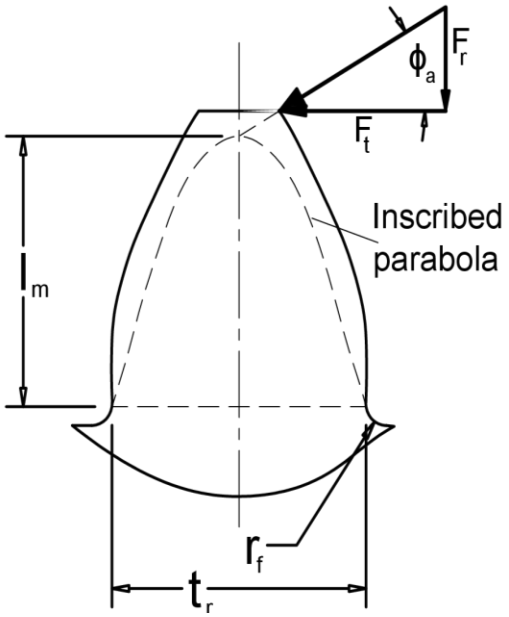

Fig: 3 Gear Tooth loading in bending

Because Archimedean worm drives is similar to a helical rack-pinion drive, pitting and bending fatigue capacities of the gear may the treated as in helical gear drives, with modifications.

6.1 Tangential and Axial Bending Stresses

In Fig. 3, the bending stress at the root of the spur gear is caused only by the tangential force. Helical gears have teeth inclined to the shaft axis that is defined by the nominal helix angle. The nominal helix angle has the effect of producing gradual gear teeth engagement, reducing transmission error in gear operations, and causing inclined contact lines on the gear tooth faces and flanks. In helical gears, the axial force also creates bending stress. Fig. 4 shows the forces on a helical gear tooth in two planes. Fig. 4a shows the loading on the y-x or transverse plane, while Fig. 4b shows the loading on the y-z or axial plane. Due to the influence of the compressive radial load in Fig. 4a, the bending moment arm of the tangential force is slightly reduced from l_m to $l_m^{/}$, the effective moment arm. Eq. (11a) give the expression for the effective bending moment arm as a function of the normal module. The root thickness of a gear tooth of involute profile may be estimated from Eq. (11b). Eq. (11c) gives the expression for the root thickness factor [13, 16].

$$l_m^{/} = \lambda_a \; m_n \qquad t_r = \kappa m_n \qquad \kappa = \sqrt{\frac{6\lambda_a}{Y_b}} \qquad (11)$$

The parameter λ_a captures the point of load application on the gear tooth profile above the critical stress point at the gear root. It locates the intersection point of the projected line of the contact force at the gear tip and the mid plane of the tooth profile perpendicular to the transverse plane as indicated in Fig. 3. A method for estimating the bending moment arm factor λ_a, for cylindrical gears using the standard rack involute tooth profile is described in [13]. The parameter λ_a is 1.8092 [13] for involute cylindrical gears of 20^0 standard pressure angle with a fillet radius of $0.375m_n$.

Expressions for the root bending stress for cylindrical and bevel gears have been developed elsewhere assuming load sharing by gear teeth and the distortion energy theory [13, 20, 21, 22]. As mentioned earlier, the distortion energy theory appears to be more realistic for worm gear bending stress. Eq. (12a) gives the expression for the root bending stress of helical cylindrical gears, while Eq. (12b) gives the stress combination factor based on the distortion energy theory.

$$\sigma_t = \frac{2K_s T \; k_\sigma k_t Y_b Y_\psi \times 10^3}{dbm_n \varpi_s} \qquad (12a)$$

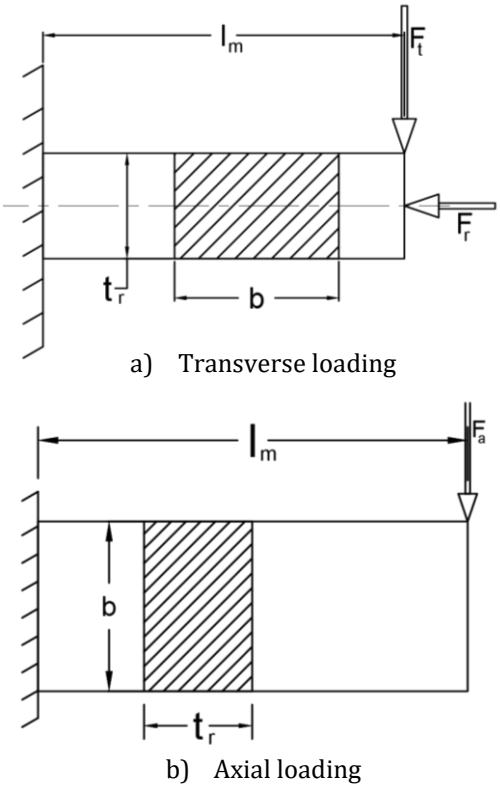

Fig. 4: Cantilever models of gear tooth in bending

$$k_t = \sqrt{\left(1 + \frac{\kappa m_n}{b}\chi_a\right)^2 + 3\left[\frac{k_\tau}{\kappa k_\sigma Y_b}\right]^2\left(1+\chi_a^2\right)} \qquad (12b)$$

The parameters T, b, d, N, k_t, and Y_b in equation (12) apply to both the pinion and gear in a mesh in cylindrical gears. In wormsets, Eq. (12a) applies to only the gear and a subscript 2 may be appended to the parameters to refer specifically to the worm gear. The Lewis stress factor Y_b for cylindrical gears in Eq. (12a) may be read from Fig. B1 using the virtual number of teeth on the gear for a known profile-shift factor. When σ_t in Eq. (12a) is higher than the fatigue or static strength of the gear material, a crack is initiated, and failure is deemed to have occurred. At low speeds, dynamic loads are low and static strength of the gear is relevant, but at high speeds, dynamic loads predominate, and dynamic strength is more relevant [3].

6.2 Stress Combination Factor (k_t)

As discussed above, bending stresses are induced by the tangential and axial load components. Helical gears, including worm gear, also experience shear stresses from the tangential and axial load components. Most of the currently available root bending stress models do not explicitly consider the shear stresses and the axial bending stress in helical gears. However, [16, 21, 22] have taken consideration of the shear stresses and axial bending stress which are encapsulated in a stress combination factor whose expression for cylindrical gears is given by Eq. (12b). The first term inside the radical in Eq. (12b) gives the sum of the tangential and the axial bending stresses at the tooth root area. The unity in the first term is associated with the tangential bending stress, while the product of the other parameters gives a factor that is associated with the axial bending stress and is usually less than unity. The second term inside the radical in Eq. (12b) is more complicated than the first term. The factor 3 is due to the assumed distortion energy failure theory used to combine normal and shear stresses. The product factor behind 3 is the normalization factor of the shear stresses with respect to the tangential bending stress. The unity in the bracketed factors of the second term is associated with the shear stress from the tangential force. The parameter χ_a is the axial force factor which is usually less than unity.

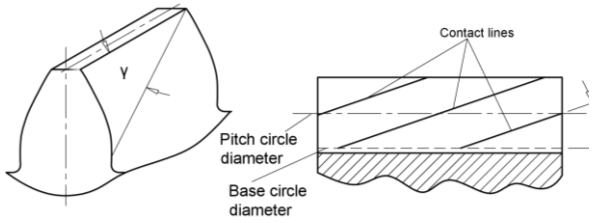

a) Contact line inclination b) Multiple contact lines

Fig. 5: Contact line inclination for helical gears [2]

The parameter k_t explicitly incorporates the additional contributions of shear stresses from the tangential and axial force components as well as the bending stress from the axial force component in the gear root bending stress in cylindrical gears. It should be noted that k_t is dependent on the nominal helix angle through the axial force factor χ_a which influences both the axial bending and shear stresses. It may be construed as an adjuster of Y_b in Eq. (12a) to partially account for the influence of the nominal helix angle of helical gears and shear stresses. The parameter k_t makes it possible for only one chart of Y_b to be used for any nominal helix angle in cylindrical gear design. This is a great simplification since different charts are not necessary for different nominal helix angles as in some gear design standards.

6.3 The Lewis Stress Factor (Y_b)

Wilfred Lewis in 1882 formulated a gear root bending stress model which in different modified forms are in national and international gear design standards [17, 23]. The model incorporated a gear form factor that is a function of the gear tooth pressure angle and number of teeth on a gear. The Lewis form factor values are available for standard gear tooth profiles only which are defined by the pressure angle. The parameter Y_b in Eq. (12a) is a modified type of the famous Lewis form factor. It is adopted from Japanese Industrial Standard (JIS) [24, 25]. For a particular standard pressure angle, Y_b is function of the virtual gear teeth number and the profile-shift factor as expressed in Eq. (13).

$$Y_b = f(\mathrm{x_n}, z_v) \tag{13}$$

Fig. B1 in the Appendix B shows a graph from which values of Y_b can read for some specific values of $\mathrm{x_n}$ and z_v. Y_b is similar to the reciprocal of the AGMA J-factor but is independent of stress concentration factor and load sharing.

6.4 Helix Angle Factor (Y_ψ)

As mentioned earlier, the influence of the nominal helix angle in helical gears is partially captured by the stress combination factor, (k_t). The contact line in helical gear mesh is diagonal on the face and flank of the gear tooth, beginning near the tip at one end to near the root at the other end [26]. Fig. 5 shows the inclination of the contact lines in helical gears [2] which creates lower root bending stress. The situation is somewhat different in wormsets where the straight contact lines on the flank and face of the gear teeth are changed to contact arcs [2] as depicted in Fig. 6. The load transmitted through contact is proportional to the arc length, and when some are not in contact, the total load transmitted is reduced.

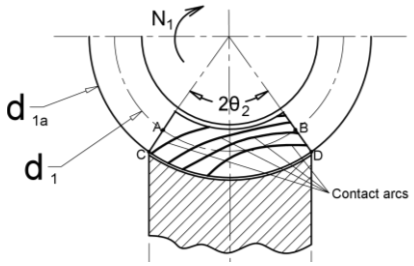

Fig 6: Contact arcs for worm-gears[2]

In cylindrical helical gears, the effect of contact lines inclination on the face of the gear teeth is accounted for by the helix angle coefficient which is given by Eq. (13a) [10, 24, 26]. However, it has been used for wormsets by Jang [10], so it is adopted here also.

$$Y_\psi = 1 - \frac{\psi}{120} \quad \begin{cases} \psi \le 30^o \\ \psi > 30^o : \psi = 30^o \end{cases} \qquad (14)$$

6.5 Stress Concentration Factors (k_σ, k_τ)

The dedendum or root circle of a gear is generally connected with the involute profile of a gear tooth with a fillet. This introduces a geometric discontinuity at the gear root area, resulting in stress concentration. Stress raisers like geometric discontinuity and scratches give rise to unusually high stresses that are quite significantly higher than the nominal values at a cross-section near the stress raisers. Eq. (12b) incorporates both normal or bending (k_σ) and shear (k_τ) stress concentration factors. A value of 1.45 for k_σ has been recommended for steel gears and appears to be satisfactory [21, 22]. Sharp fillets are to be avoided in steel and polymer products [27] to minimize stress concentration. Plastic materials are quite notch sensitive like steel materials, but their response to fatigue loading is not as well understood as that of steel material, so a value of 1.55 for k_σ is suggested. According to Dobrovolsky et al [5], the normal stress concentration factor for cast iron gears is about 1.2 and a design value of 1.25 is suggested for cast iron and non-ferrous gear materials due to their relatively low sensitivity to stress concentration effects. The shear stress concentration factor k_τ is in general a function of material and geometry like the normal stress concentration factor. It ranges from 1.6 to 2.2 for harmonic gears that are manufactured with similar tools used for cylindrical gears [28]. The value of k_σ for cast iron and non-ferrous materials is at the lower range, so the value of k_τ is expected at the lower range too.

Therefore, a value of 1.75 is suggested for k_τ for worm gears of cast iron and non-ferrous materials. For steel and plastic materials, a value of 2 for k_τ is recommended. Table 1 summaries stress concentrations factors for worm gear applications.

Table 1: Stress Concentration Factors

Worm Gear Material	k_σ	k_τ
Cast irons and copper alloys	1.25	1.75
Steels	1.45	2.00
Plastics	1.55	2.00

7.0 LOAD SHARING FACTOR (ϖ_s)

In wormsets, the number of pairs of gear teeth sharing the transmitted load is usually higher than that for cylindrical helical gears. In cylindrical gears, the number of pairs of gear teeth in simultaneous contact in a mesh is seldom more than 2. During gear transmission 2 to 3 gear teeth are claimed to be in contact with threads in wormsets [18]. The average number of teeth in mesh is represented by the contact ratio. In order to have more than 2 or 3 gear teeth sharing the transmitted load in wormset meshes, the expression for the virtual contact ratio (ϖ_v) used for cylindrical gears has to be modified due to number of threads in a worm and the number of gear teeth enclosed by the effective facewidth of the worm. Therefore, the contact ratio in wormsets is construed to have two components of the basic virtual contact ratio (ϖ_v) and worm contact coefficient (λ_c) [15, 29].

7.1 Virtual Contact Ratio

The virtual contact ratio is the average number of pairs of gear teeth simultaneously in mesh on the virtual plane during operation. Eq. (15a) gives the virtual contact ratio and Eq. (15b) gives the contact recess factor [29, 46].

$$\varpi_v = \frac{\kappa_1 + \kappa_2}{\pi \cos\phi_n} \qquad \kappa_1 = \frac{1}{\sin\phi_n} \qquad (15)$$

Eq. (16) gives the contact approach factor [29, 46].

$$\kappa_2 = 0.5\left\{\sqrt{(z_{v2}+2))^2 - (z_2\cos\phi_n)^2} - z_{v2}\sin\phi_n\right\} \qquad (16)$$

7.2 Worm Contact Coefficient (λ_c)

A thread groove on a worm may be considered as a pathway for the teeth on a worm gear. More than one gear tooth is normally in contact with the worm thread. The depth of contact of each gear tooth in the mesh with a thread varies [18]. When there are multiple threads on a worm, the chances of two or more gear teeth being in mesh simultaneously increase because each thread provides a separate pathway for the gear teeth meshing. The contact path between a worm thread and a gear tooth is curved and inclined relative to the tooth root as shown in Fig. 6. The contact zone is defined by the effective facewidth of a worm thread and it encloses several gear teeth that can mesh with available thread pathways.

The worm contact coefficient (λ_c) and worm contact effectiveness factor (α_e) are used to capture the complicated interaction between the number of enclosed gear teeth and the number of threads on a worm [15, 29]. Eq. (17a) gives the estimate of the number of gear teeth in the contact zone, while Eq. (17b) is the expression for the worm contact coefficient where a trailing and a leading tooth are assumed to be non-effective.

$$n_g = \frac{b_1}{\pi m_n \cos\psi} \qquad (17a)$$

$$\lambda_c = \sqrt{\alpha_e \left(n_g - 2\right) z_1} \geq 1.0 \qquad (17b)$$

The worm contact effectiveness factor (α_e) is assumed to account for the summation of the series of arcs of contact between the gear teeth faces and worm threads because the transmitted load is proportional to the length of the arcs shown in Fig. 6. It is estimated that $0.4 \leq \alpha_e \leq 1.0$ for cylindrical worms [29]. The average value of 0.7 is chosen for this study; however, a value of 0.75 is suggested by Petrov et al [2,].

The theoretical contact ratio for cylindrical worm gears is the product of the virtual contact ratio (ϖ_v) and the worm contact coefficient (λ_c) which is given by Eq. (18a).

$$\varpi_c = \varpi_v \lambda_c \qquad \varpi_s = 1 + 0.80\left(\varpi_c - 1\right) \qquad (18)$$

Ideally, the theoretical contact ratio should represent the load sharing factor. However, shaft deflections, gear deformation, and the deformation of gear drive supporting members tend to lower the theoretical contact ratio. Generally, load sharing can be enhanced by wear-in and accurate manufacture of gear teeth. Inaccurate low-hardness gears may wear-in and cold-flow enough to develop relatively good contact patterns, allowing better load sharing early in their service life [11]. Load sharing is critical to noise, vibration, efficiency, strength, wear, and life of gears. Higher contact ratio lowers the noise and increasing the overlap ratio in helical gears will also reduce the noise. But low manufacturing accuracy and high hardness of gear teeth reduce load sharing. The theoretical contact ratio must be above unity for practical reasons and ensuring proper function of gears with lower contact ratio requires higher accuracy in manufacturing and assembly. Therefore, the minimum theoretical contact ratio usually recommended is 1.2 [18]. Now the reciprocal of 1.2 is 0.833 which may be used to adjust the theoretical contact ratio for a gearset in estimating the load sharing factor. Due to the complexity of the geometry and kinematics of wormsets, Eq. (18b) is suggested for estimating the load sharing factor for cylindrical worm gears.

Eq. (18b) is taken as the predictor of the expected number of worm gear simultaneously in contact with the thread(s) on a worm practically. It is a derated value of the theoretical virtual contact ratio. The parameter λ_c has a value that is at least unity, therefore Eq. (18b) will give estimates of higher values than that for cylindrical helical drives of the same worm gear teeth number.

7.0 WORM GEAR PECULIAR FEATURES

Worm gears are special helical gears with some specific features that distinguish them from helical cylindrical gears. When worm gears mesh with worm threads, the gear teeth move along helical troughs with the faces of the threads acting as guides. This somewhat constrained motion is completely absent in helical cylindrical gear meshes. It, however, provides some enhanced rigidity to worm gear teeth that helical cylindrical gear teeth do not have. Also, the geometry of the gear teeth in worm gears is not uniform across the facewidth as in helical cylindrical gears [30].

Other features that make worm gears special compared to helical cylindrical gears include throating, mode of tangential load application, variable apparent pitch diameter of worm gear in mesh, and worm gear tooth backlash. Cylindrical worm gears are usually throated, a feature absent in helical cylindrical gears. Secondly, the direction of the tangential load in worm drives is not fixed but moves along an arc on the pitch circle diameter of the worm. Therefore, the path of resistance to the load is an arc that is longer than the worm gear facewidth. Thirdly, the motion of

the tangential load along the arc of the worm diameter circle suggests that the apparent pitch diameter of the gear is variable during meshing. Fourthly, backlash in wormsets is usually applied on the worm thread thickness, making the gear teeth slightly thicker than that of helical cylindrical gears. These features make it not possible to generate an exact solution for the root bending stress of worm gears. Practically, they call for a modification of the basic root bending stress model for helical cylindrical gears given by Eq. (12a). Therefore, the expression for the root bending capacity for worm gears may be taken as in Eq. (19a), incorporating an effective stress adjustment factor for worm gear features that may be obtained from Eq. (19b).

$$\sigma_t = \frac{2K_s k_\sigma k_t Y_{b2} Y_\psi T_2 \times 10^3}{\beta_o \varpi_s m_n b_g d_2} \qquad \beta_o = \beta_1\beta_2\beta_3\beta_4 \qquad (19)$$

7.1 Gear Throating Stress Factor (β_1)

When a power screw is mated with a gear of the same axial pitch as in Fig. 7a, a straight wormset is formed. Themeshing between the screw and the gear is approximately a point contact and the load capacity is severely limited. Practically, the elastic deformation of the gears and supports converts the point contact into a circular patch which gives rise to high Hertz contact stresses. However, if the gear is cut with a hob in the shape of the power screw that simulates the motion of the worm against the gear, the meshing between the worm and the gear becomes approximately a line contact [31]. The hob cutter creates a curvature on the gear teeth surfaces that is described as throating and gives the appearance shown on the right figure in in Fig. 7b. The number of threads on the hob for making the worm gear

should match the number of threads on the worm. The concave profile of the gear produced by throating in cylindrical worm gears allows the gear to wrap around the worm threads thus ensuring better contact and meshing effectiveness. This results in better load distribution in the mesh and reduces local contact stresses. Therefore, the induced bending stress at the root of the gear is more evenly distributed. The gear tooth is restrained to some extent due to throating, giving it more stability [5]. Throating benefits are realized in wormsets when the housings are manufactured accurately and gearset is properly aligned during installation. The middle plane of the worm gear should pass through the axis of worm. After the worm drive is installed, it may need axial position adjustment to ensure proper meshing with the worm. Also, maintaining proper center distance and shaft angle are critical so that proper wrapping can occur between the gear teeth and worm thread(s). Improper mounting and misalignment may create point contact instead of line contact, resulting in high contact stress that can lead to premature failure of the wormset. Throating worm gears enhances line contact during meshing in cylindrical wormset, making the contact pattern similar to that of cylindrical gears. Since Eq. (18a) is a modification of the root bending stress model of helical cylindrical gears where line contact occurs, the throating factor for cylindrical wormsets is assumed to be unity. That is $\beta_1 = 1.0$ in this study.

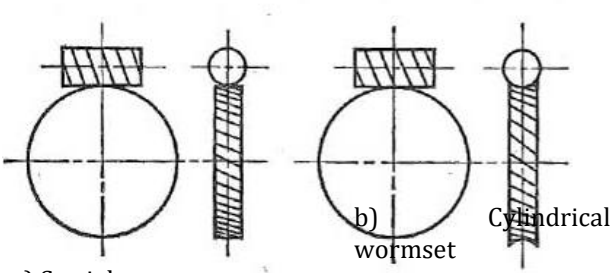

a) Straight wormset b) Cylindrical wormset

Fig. 7: Wormsets [27]

7.2 Worm Load Path Stress Factor (β_2)

Unlike helical gears with a tangential force component that has a fixed direction during meshing, the tangential force of worm gears moves along the arch AB on the pitch circle diameter of the worm as shown in Fig. 8. Thus, the direction of the tangential

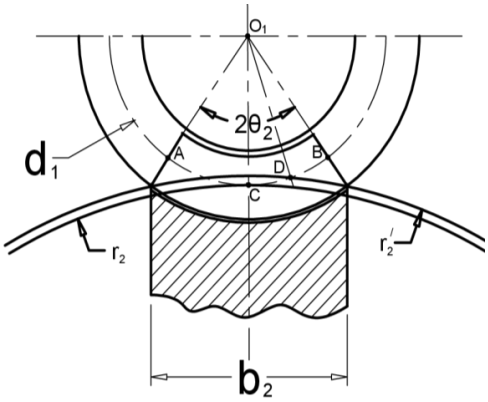

Fig 8 Load arc profile

force changes continuously when the worm gear and worm thread(s) are in mesh. In spiral bevel gears, where the tangential force has a fixed direction, it is known that the curvature of the spiral bevel gear tooth helps to strengthen the gear tooth against bending failure [18, 32, 33]. The contact surface in the case of spiral bevel gears is an arc, but worm gears have straight teeth. However, the applied tangential load moves in a circular path along the arc AB in Fig. 8. Hence by analogy with spiral bevel gears, the situation

$$y = 0.5d_1\left(1-\cos(0.5\theta_2)\right) \qquad r_2^{/} \approx r_2 + y \qquad (22)$$

in worm sets seems to be a mirror image of spiral bevel gears. Therefore, it may be argued that the arc indicated by points A and B on the worm pitch circle diameter in Fig. 8 is the resisting portion of the gear facewidth against the tangential force. Hence, the worm gear is strengthened against bending resistance as is the case in spiral bevel gears [22]. The arc CD in Fig. 8 is on the dedendum circle diameter of the gear which is close to the critical section in the root area. Hence the arc CD is approximately the effective arc length resisting the bending load. According to [5], the increase in tooth bending resistance of the worm gear teeth may be assumed to be proportional to the relative length of arc CD to AB [5]. The arc CD is close to addendum radius of the worm plus the clearance allowance on the gear. Therefore, the strengthening factor may be approximated as given in Eq. (20a).

$$\beta_2 = \frac{d_{a1}+2c_f}{d_1} = \frac{d_1+2m_n(1+c_f)}{d_1} \qquad d_1 = z_w m_a \qquad (20)$$

Combining Eq. (20a) and Eq. (20b) gives Eq. (21a). The clearance factor c_f is 0.20 for ISO worm gears and $z_w = 10$ is considered an average value [2, 5] for cylindrical worm gear. Thus, the arc load strengthening factor may be evaluated as in Eq. (21b) as an average value.

7.3 Worm Arc Profile-Shift Stress Factor (β_3)

$$y = x_p m_n \qquad x_p = 0.5z_w\left(1-\cos(0.5\theta_2)\right) \qquad (23)$$

Consider Fig. 9, where the pitch radius of the worm gear is defined on the central plane O_1C of the worm. The contact envelope is $2\theta_2$ and it is the total face-angle of the gear. On the central plane O_1C, the pitch radius of the gear is r_2. To the left and right of the central plane, a gear tooth apparent pitch radius depends on the section in the worm contact envelope angle measured from the plane O_1C. It increases as the angle increases from the central plane O_1C to line O_1A or line O_1B. This can be observed on the axial plane of the worm which corresponds to the diametral plane of the gear, but the dimensions of the pitch radius of the gear in the diametral plane may be superimposed on the axial plane of the gear as indicated in Fig. 9. For instance, at point D on the worm pitch circle diameter, the apparent pitch radius of the gear is represented by $r_2^{/}$. If the line O_1D is chosen to be midway between lines O_1C and O_1B, point D may be taken as representing the average of the change in the apparent pitch radius of the gear during engagement with the worm. When the contact point on a gear tooth is at point D, the vertical distance between points C and D is given by Eq. (22a). The apparent pitch radius of the gear at point D is given, approximately by Eq. (22b).

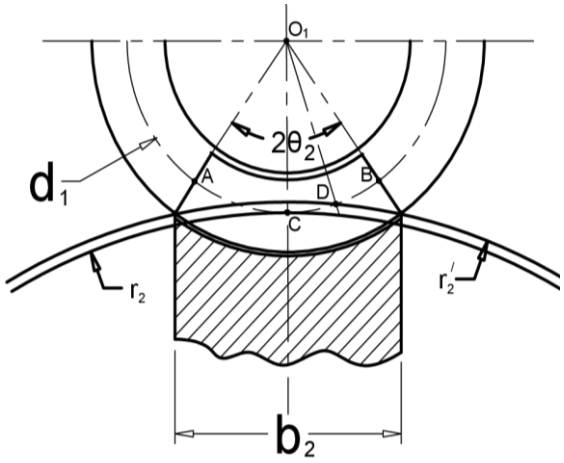

Fig 9: Worm gear apperent pitch radius

$$\beta_2 \approx 1+\frac{2(1+c_f)}{z_w} \qquad \beta_2 \approx 1+\frac{2(1+0.2)}{10} = 1.24 \qquad (21)$$

In Fig. 9, the apparent increase in the pitch radius of the gear may be associated with an apparent profile-shift factor as expressed in Eq. (23a). When Eq. (22a) and Eq. (23a) are combined, the apparent profile-shift factor is obtained from Eq. (23b).

According to Dobrovoslky et al [5] and Petrov et al [2], the gear face-angle is approximately $2\theta_2 = 100^o$, for which from Eq. (23b), gives a value of $x_p \approx 0.5$. The apparent profile-shift factor is positive because it increases the pitch radius of the gear. A positive profile-shift factor strengthens gear tooth against bending resistance. For a worm gear of a specific number of teeth, the increase in the bending resistance will the ratio of the Lewis stress factor for $x_p \approx 0$ and $x_p \approx 0.5$ from Fig. B1. In power drive wormsets, the number of teeth on the gear could be between about 21 to 100 and the increase in the Lewis stress factor in cylindrical worm gears due to $x_p \approx 0.5$ is in the range of 1.06 to 1.28, which gives an average value of $\beta_3 = 1.17$.

7.4 Gear Tooth Thickness Stress Factor (β_4)

Fig. 10 depicts the use of backlash in a gear mesh which is the intentionally provided clearance between mating gear teeth. It is crucial for preventing binding, accommodating

thermal expansion, accommodating manufacturing, and assembling inaccuracies, and providing space for lubricants. However, backlash is minimized in precision applications like robotics and indexing drives. The actual thickness of helical gear teeth in mesh is very slightly reduced by the applied backlash because it is subtracted from the gear tooth thickness. But the backlash for a wormset mesh is subtracted from the worm thread thickness, not the worm-gear tooth thickness [34]. This makes cylindrical worm gear tooth thickness slightly more than that of regular cylindrical helical gears. Eq. (24a) is a backlash expression, Eq. (24b) expression is for the backlash factor,

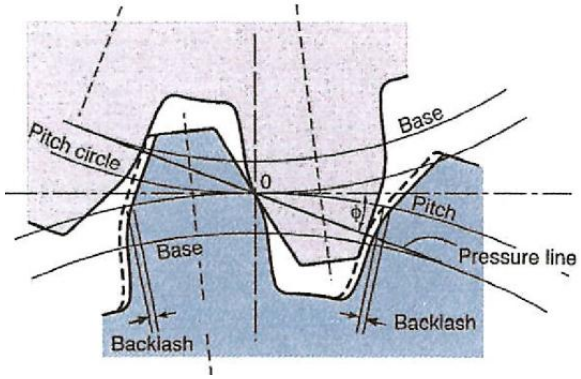

Fig. 10: Backlash in gear mesh [18]

$t_b = \alpha_b m_n$	$\chi_b = 1 \pm \frac{2\alpha_b}{\pi}$	(24)

The '+' sign in Eq. (24b) is used when the backlash is added to the gear tooth thickness and the '-' sign is used when it is subtracted.

$t_a = 0.5\pi m_n \chi_b$	$\beta_4 = \chi_b^2$	(25)

Eq. (25a) expression is for the circular tooth thickness, and Eq. (25b) expression is for the gear tooth thickness factor. Since the bending stress resistance is proportional to the square of the root thickness, the approximate stress increment or reduction factor is given by Eq. (25b). In most gears, the backlash is subtracted and the parameter χ_b is less than unity. When the backlash is added to the gear tooth thickness, as in worm gears, the parameter χ_b is greater than unity. Generally, worm gears require more backlash than cylindrical gears duce to differential expansion between steel worms and bronze worm gears [11]. Worm gears are produced with a backlash range of ±0.045m_n [35]. However, the minimum normal backlash for industrial gears is in the range of 0.03m_n to 0.04m_n [36]. Assuming an average normal backlash of 0.04mn (α_b 0.04) for worm gears, the parameter χ_b of Eq. (24b) will be 1.0255 which leads to an approximate stress reduction factor (Eq. (25b)) of $\beta_4 = \chi_b^2$ = 1.052 for cylindrical worm gears.

From the above considerations of stress adjustment factors for cylindrical wormsets, Eq. (19b) be evaluated as in Eq. (26).

$$\beta_o = 1.0 \times 1.24 \times 1.17 \times 1.052 \approx 1.53 \quad (26)$$

The effective stress adjustment factor β_o for cylindrical worm gears is estimated to be approximately 1.53 on the average. The reciprocal of β_o is 0.66, which suggests that the root bending stress for a cylindrical worm gear is about 66% that of a cylindrical helical gear of the same size and basic proportions under similar loading. Therefore, a cylindrical worm gear has 34% higher root bending stress capacity than an equivalent cylindrical helical gear.

8.0 Worm Gear Root Bending Stress Capacity

The root bending stress capacity of a gear is the maximum tensile stress it can satisfactorily resist without the initiation of a crack or yielding. Crack initiation is often of fatigue origin, while yielding may be caused by static overload, but both may be caused also by momentary overload. With a numerical estimate of β_o available from Eq. (26), the root bending stress model expression for helical cylindrical gears of Eq. (19a) can be modified as in Eq. (27) to obtain that for cylindrical worm gears.

$$\sigma_t = \frac{2K_s k_\sigma k_t Y_{b2} T_2 \times 10^3}{1.53 \varpi_s m_n b_g d_2} \quad (27)$$

When Eq. (27) is simplified, Eq. (28) is obtained. This becomes the new expression for the root bending stress capacity for cylindrical worm gears.

$$\sigma_t \approx \frac{1.35K_s k_\sigma k_t Y_{b2} T_2 \times 10^3}{\varpi_s m_n b_g d_2} \quad (28)$$

The above analysis shows that the maximum stress at the root of a cylindrical worm gear is about 66% of that of a helical cylindrical gear. The strength increase in cylindrical worm gears comes mainly from the throating of the worm gear due to stress factors β_2 and β_3 .

9.0 Root Bending Stress Model Applications

The bending stress capacity model of Eq. (28) for cylindrical worm gears is tested in a set of five gear design examples taken from different references. Example 1 is taken from KISSsoft tutorials [37]. KISSsoft is a commercial software which is developed by a subsidiary of Gleason Corporations, a renowned gear manufacturer in the United States and developer of gear standards. It provides engineering solutions in gear technology and other design areas and is increasingly becoming popular in the industry. Example 2 is from MITCalc works [38], a software suite for mechanical engineering, industrial and technical calculations. It is of European origin and may be a modified version of ISO or a proprietary standard. The solutions from this software are considered accurate and reliable. Example 3 [2] and Example 4 [39] are taken from textbooks of Russian origin, so the root bending stress design models are probably from or modifications of GOST design standards of the former Soviet Union. Example 5 [10] is taken from a textbook of Chinese origin, and the root bending stress design model is likely from GB (People's Republic of China) gear design standard or a modification of it. KISSsoft, MITCalc, and GB standards are newer than the GOST standards. Example 1 to Example 4 have profile-shift factor of 0, but Example 5 has a profile-shift factor of -0.5.

The new root bending stress model expressions for cylindrical worm gears were coded into Microsoft Excel for the design analysis of the root bending stresses of the wormsets in the cited references. The input data for the design examples are provided in Table 2. Table 3 gives some intermediate data for evaluating the root bending stresses for the design examples. Table 4 shows the components of the service load as evaluated using the method of Appendix A for the design examples. It also shows the service load factors from the cited references and those obtained based on Appendix A. Table 5 provides the evaluated root bending stresses for the examples using the service load factors in the cited references. It also compares the current stress estimates with the previous values. Table 6 gives the evaluated root bending stresses for example using the service load factors based on Appendix A method. It also compares the current stress estimates with the previous value.

Table 3: Computed Data for Application Examples

Example	ϖ_v	λ_c	ϖ_c	ϖ_s	k_t	V_s	q_n
EX1	1.856	1.738	3.225	2.780	1.229	2.896	9
EX2	1.903	1.883	3.583	3.067	1.205	5.796	7
EX3	1.833	1.499	2.748	2.399	1.219	6.304	7
EX4	1.828	1.537	2.810	2.448	1.179	4.110	8
EX5	1.852	1.664	3.083	2.667	1.162	6.242	7

Table 4: Load Influence Factors and Service Load Factor

Parameter	EX1	EX2	EX3	EX4	EX5	Average
Application factor (K_a)	1.000	1.000	1.000	1.000	1.000	1.000
Internal overload factor (K_v)	1.152	1.109	1.113	1.132	1.113	1.124
Mesh overload factor (K_m)	1.090	1.126	1.109	1.106	1.099	1.106
Frictional overload factor (K_f)	1.033	1.025	1.026	1.029	1.024	1.027
Worm type load factor (K_w)	1.000	1.000	1.000	1.000	1.000	1.000
Service load factor (K_s)*	1.298	1.279	1.266	1.288	1.253	1.277
Service load factor (K_s)**	1.000	1.000	1.100	1.200	1.210	-
* Service load factor estimated using new model			**Service load factor from references			

Table 5: Matched K_s Root Bending Stresses and Comparison

Example	Current	Previous	Dev (%)
EX1	47.53	61.51*	-22.72
EX2	56.52	83.47*	-32.29
EX3	7.36	9.00	-18.27
EX4	6.84	7.11	-3.83
EX5	12.65	13.79	-8.23
*Shear stress converted to normal stress based on distortion energy theory			

Table 6: Unmatched K_s Root Bending Stresses and Comparison

Example	Current	Previous	Dev (%)
EX1	61.83	61.51*	0.51
EX2	72.41	83.47*	-13.25
EX3	8.47	9.00	-5.90
EX4	7.28	7.11	2.34
EX5	13.29	13.79	-3.65
*Shear stress converted to normal stress using distortion energy theory			

10.0 DISCUSSIONS

The root bending stress capacity of a gear is the maximum tensile stress it can satisfactorily resists without the initiation of a crack or yielding. Reliable operation of gears requires that the root bending stress must be less than the fatigue or yield strength of the gear material. Fatigue strength is relevant in fatigue loading while the yield strength is relevant in static condition. Therefore, a reasonably accurate root bending stress capacity model is necessary to ascertain the adequacy of a gear design, especially when the bending strength is critical for functional and reliable operation.

The worm gear root bending stress capacity model of Eq. (28) is unique when compared with current gear design models because of the parameters k_t and ϖ_s. The parameter k_t accommodates both the normal k_σ, and the shear k_τ stress concentration factors, a feature not present in any current gear design model. It may be construed as a modifier of the Lewis stress factor. The most important advantage of k_t is that it allows the value of Y_b for a spur to be used for any helical gear of any nominal helix angle. This eliminates the need of different Y_b design charts for different nominal helix angles, thus, simplifying gear design analysis.

The values of k_σ and k_τ are purely properties of the gear material and fillet size at the gear root. They are completely decoupled from the Lewis stress factor and are also independent of the load application point on the gear tooth profile during meshing. The gear material for the design examples is bronze, and the values of k_σ and k_τ used in the stress estimates are 1.25 and 1.75, respectively, as recommended earlier.

The parameter ϖ_s represents the load sharing capability of a wormset which is a derated value of ϖ_c (Eq. (18)). The parameter ϖ_c is the theoretical contact ratio which is evaluated as the product of the virtual contact ratio ϖ_v of a helical rack-gear mechanism and a worm contact coefficient λ_c (Eq. (17b)). The parameter λ_c is particularly important because it is used to capture the complex contact patterns between worm threads and gear teeth during

wormset operation. It is a function of the number of threads on a worm z_1 , the number gear teeth in the contact zone, n_g (Eq. (17a)), and the contact effectiveness factor α_e .

The parameters λ_c , n_g , and α_e are all new parameters introduced into worm gearing design analysis elsewhere [15, 29]. Current worm gear design models appear not to have these parameters in the root bending stress analysis. λ_c has a minimum value of 1.0 and α_e has a value in the range of 0.4 to 1.0, based on common worm design practice currently [15, 29]. The average value of 0.7 is used in this study and is the recommended value.

When the new root bending stress model was used in the examples for stress estimation, the normal module, the pitch diameter of the worm, the pitch diameter of the gear, the gear facewidth, and the worm facewidth were those from the references. The solutions were evaluated afresh as decisions of profile quality are different from those in some of the references. The decision to use different profile quality grades was informed by the desire to ensure consistency in gear profile quality grades associated with the sliding speed. The gear profile quality grade is influential in determining the value of the internal overload factor for a gearset. In the root bending stress analysis, the gear tooth profile accuracy grade was selected so that the basic or spur gear internal overload factor K_o is at most 1.25.

Table 2 column 2 gives the nominal torque on the gear in a range of 200 to 10,000 Nm which is more than one order of magnitude. Column 3 of Table 2 gives the pitch diameter of the gears in the range of 160 to 500 mm, approximately, while column 4 gives the pitch diameter of the worm in the range of 35 to 100 mm. The speed ratio is given in column 5 and is roughly in the range of 15 to 25. Column 6 gives the number of threads on the worms, with four worms having a value of 2, and one has a value of 3. The nominal facewidth of the gear is given in column 7 and is in the range of 30 to 80 mm, while the nominal facewidth of the worm is given in column 8 with a range of 60 to 200 mm, approximately.

Table 3, column 2 gives values of the virtual contact ratio, which are observed to be above 1.80, depending on the number of teeth on the gear. The values of the worm contact coefficient are in column 3 in Table 3 and they are in the range of 1.5 to 1.9. They are estimates of the likely theoretical increase in load sharing resulting from the use of multiple threads and from the number of gear teeth enclosed in the contact zone. The values of the theoretical contact ratio are provided in column 4 of Table 3 and are in the range of 2.75 to 3.60, approximately. Table 3 column 5 shows the load sharing factor which represents the expected contact ratio. This column indicates that 2 to 3 gear teeth are in contact with the worm threads during load transmission for design examples 1, 3, 4, and 5. For design example 2, 3 to 4 gear teeth are in contact during wormset operation. Comparing these load sharing factors with column 6 of Table 2, they are more than the number of threads on the worm. This implies that a worm may accommodate at the least one gear tooth in a worm thread simultaneously in operation. This is not unreasonable physically since each thread provides a separate pathway for gear teeth motion. The evaluated number of gear teeth in engagement agree with the observation of Hamrock et al [18], who said two or more gear teeth are in mesh in wormsets during operation.

Table 3, Column 6 provides values of the stress combination factor evaluated for the design examples. There is little variation in the values of this parameters in these examples, indicating its low sensitivity to different gear deign parameters. Table 3, Column 7 gives the calculated sliding velocity for the wormset, while column 8 gives the International Standardization Organization (ISO) gear profile quality number used in evaluating the basic internal overload factor. It is worth noting the relative consistency of gear quality number and sliding speed in the wormsets in columns 7 and 8 of Table 3. This is expected practically since higher quality grades are required for higher sliding speeds.

Table 4, column 2 shows the service load factor component values for each design example as evaluated using the method summarized in Appendix A. The values are provided in rows 2 to 6 of the table. In row 2 of the table, the application factor is chosen to be 1.0. The values of the internal overload factor are between 1.1 and 1.16 in row 3. The values of the mesh overload factor in row 4 are between 1.09 and 1.13. The values of the frictional load factor in row 5 are between 1.024 and 1.033, with lower values associated with higher sliding velocities. In row 6 of the table, the worm type load factor is 1.0 because ZN thread type was assumed for all examples. Row 7 of the table provides the service load factors for each design example based on the evaluated components using Eq. (10) or Eq. (A1). The values are in the range of 1.25 and 1.30, with an average 1.28 as indicated in column 7 of the table. This shows that the nominal load is not increased more than about 30% inside these wormsets for a load application factor of unity in these design examples. Such low overall internal load increases is expected of wormsets as they are said to be the quietest of gear drives [42]. Row 8 of Table 4 provides the service load factors deduced from the cited references.

Table 5, column 2 shows the root bending stress estimates from the new model using the same design sizes and service load factors (row 8 of Table 4) in the cited references.

Therefore, the stresses in column 2 of Table 5 can be directly compared with those from the references shown in column 3 of the same table. The stresses for example 1 and example 2 in column 3 of Table 5 were provided as nominal root shear stresses of 35.51 MPa and 48.25 MPa in [36] and [37], respectively. Assuming von Mises or distortion energy failure rule for ductile materials, the normal stress values become 61.50 MPa and 83.57 MPa, respectively as shown in Table 5. Table 5 column 4 shows the percentage variances between the stress estimates from the new model and previous results. These variances are between -32.3 and -3.8% with the larger deviations being in examples 1 and 2. It should be recalled that the previous solutions for these examples were based on the nominal shear stress criterion which is considered conservative [4]. Since the deviations are all negative, the previous solutions seem conservative relative to the new model solutions. This is not unexpected because the root bending models in the references do not incorporate all the design parameters of a wormset as the new model. It is often the case that models tend to be conservative when there is ample uncertainty in a design situation. Wormset design does have quite some uncertainties which the study has tried to reduce.

Table 6 column 2 shows the root bending stress estimates from the new model using the same design sizes as in Table 5, and the service load factors of row 7 of Table 4. The service load factors were evaluated using the method of Appendix A based on Eq. (10) or Eq. (A1) for the design examples. The values are different from those in the cited references (row 8 of Table 4). Therefore, the stresses in column 2 of Table 6 are the solutions based on the new root stress model and the service load factor of the method in Appendix A, which may be seen as new solutions all together. They are compared with those from the cited references shown in column 3 of the same table and the percentage variances between the stress estimates are provided in column 4. The variances between the current and previous results are approximately between -13.3% and 2.4%. The negative variances show that the new model estimates are lower than the previous values, while positive variances show the new model values are higher than the previous values. The variances appear not to be unreasonable considering the fact that the previous estimates are deemed conservative. It should be noted that the method used for evaluating the service load components in Appendix A is similar to those used for cylindrical and bevel gears [12, 13, 19, 20, 26]. Thus, the method proposed in Appendix A brings a consistency level in gear design technology not present before now.

The expression used for estimating K_m (Eq. (A5a)) in Appendix A was taken from Hamrock et al [18] and adapted to cylindrical wormset application with some modifications using the gear parameters instead of those of the pinion in the original expression. It was assumed that K_v may be substituted for K_m when estimating K_A to avoid an iterative solution for K_s and K_m. In the original expression for K_m in [18], K_a is used instead of K_A. The load application factor K_a, accounts for only the load increases caused by external masses connected to a gear drive. But actual deflection and distortion of gears and supporting structures, which determine the actual value of K_m, are caused by the service load that is estimated with K_s. Since K_s has K_m as a component in its evaluation in Eq. (10) or Eq. (A1), the two parameters must be solved iteratively to have a valid solution, if K_s is used in Eq. (A5a). This was avoided by introducing the parameter K_A where K_v was used to replace K_m. Therefore, K_s and K_A should be about the same in values.

Table 7 is provided to validate that assumption in Eq. (A5a). As can be observed, the values of K_a in column 2 are considerably lower than those of K_s in column 3. This implies that the deflection and distortion of structural members in a gearbox may be underestimated if K_a is used instead of K_s. Column 4 of Table 7 shows the values of K_A and column 5 shows its percentage deviation from K_s. The range of the variances in column 5 of Table 7 is between -1.53 to 5.66% which seems to be very small and marginally conservative. Therefore, the assumption in Eq. (A5b) is reasonable and validated.

Table 7: Comparison of K_s and K_A

Example	K_a	K_s	K_A	Dev. (%)
EX1	1.000	1.298	1.371	5.66
EX2	1.000	1.279	1.260	-1.53
EX3	1.000	1.266	1.271	0.36
EX4	1.000	1.288	1.318	2.33
EX5	1.000	1.253	1.268	1.20

The components of the parameter K_s and the parameter λ_c differentiate the new root stress model distinctively from others available. The parameter components K_w and K_f of K_s are also unique, being absent in other models available. K_w takes care of the worm thread profile type and varies between 0.6 and 1.0 (Table A4) and

the applicable value in this study is 1.0 for ZN thread profile. K_f takes care of the additional load resulting from the presence of friction in the gear and screw meshes. As a modifier of ϖ_c, the parameter λ_c makes it possible to estimate a more realistic load sharing factor for cylindrical wormsets. Considering all these factors, it is remarkable that the root bending stresses of Table 6 column 2 compare very well with those in the references as indicated in Table 6 column 3.

Four (4) stress adjustment factors were considered for a worm gear in Eq. (19b). Three (3) are associated with the throating of the worm gear and the fourth is due to the backlash allowance for worm gears. The numerical estimates for these factors are $\beta_1 = 1.0$, $\beta_2 = 1.24$, $\beta_3 = 1.17$, $\beta_4 = 1.052$, and their product is $\beta_o = 1.53$. The factors β_1, β_2, and β_3 depend on worm gear throating which contributes 94.82% to β_o. With $\beta_o = 1.5$, the root bending stress in a worm gear is reduced to about 66% of that of a cylindrical helical gears of the same size. Thus, worm gears have about 34% higher root bending stress capacity than equivalent cylindrical helical gears under the same loading conditions.

Helical cylindrical gears have a constant tooth section in the axial direction as opposed to the somewhat variable section of worm gears, as mentioned earlier [30]. The variable tooth section of a worm gear may well have some influence on the contact stress capacity of a wormset, but any influence on the beam strength capacity is doubtful. This is because, the gear root section is rectangular in shape and the thickness which largely determines the beam strength capacity of a gear tooth has little or no variation at gear root section. The gear root thickness is fairly uniform once a gear is manufactured. Throated worm gears have a reduced tooth height around the central axial plane. The reduced tooth height is somewhat similar to gear stubbing which is sometimes used to strengthen the beam strength of gears [18]. However, the effect of stubbing is not examined in this study but it is a possible area of exploration and improvement on the current model.

The true bending stress at the root of a gear tooth is not easily determined. Gear design technology using Finite Element Method (FEM) and Boundary Element Method (BEM) can determine more accurately, the local strain and stress states in the root area when actual geometry of both gear teeth and body are used [4, 40]. FEM is generally time consuming, requiring considerable computer resources than BEM. FEM and BEM require special computational skills and experience. But, BEM and FEM require initial gear teeth and body dimensions that can be generated using approximate stress capacity models like the one presented. The new model is quite analytical and scientific and contains fewer uncertainties compared to those in current use. The complex state of stress at the gear root, especially that of a worm gear, suggests that approximate stress capacity models should be somewhat conservative in order to minimize the chances of gear failure and provide reasonable service life. The new model predictions compare very favorably with earlier conservative estimates. Consequently, it appears quite satisfactory, and may help to cut down on the time and resources used during optimization with FEM or BEM analysis if used for initial design. This is due to the fact that the model provides more detail analysis with reduced uncertainties.

11.0 CONCLUSIONS

A root bending stress expression is derived for cylindrical wormsets by considering the worm as a helical rack mating with a helical gear. The concept of equivalent spur gear for a helical gear defined by the instantaneous radius of curvature in the virtual plane of the helical gear is utilized in the bending stress capacity model formulation. The virtual plane is defined by the base helix angle and is different from the normal plane which is defined by the nominal helix angle. According to Maitra [6], the instantaneous radius of curvature of the equivalent spur gear of a helical gear is estimated more accurately on a virtual plane defined by the base helix angle.

The new model uses all the basic design parameters of worm and gear found in current models and incorporates new ones such as the worm contact coefficient and contact effectiveness factor. The last two parameters are used to capture the complex meshing condition in wormsets and allows the model to account for multiple threads in worms and the number of gear teeth in the contact zone. Appendix A provides a summary of a method that may be used to evaluate the load service factor for wormsets. It modifies the service load factor expression for cylindrical gears by taking account of different thread profile designs in wormsets and the influence of mesh friction.

The new cylindrical worm gear root bending stress model was developed from that of cylindrical helical gears by defining four stress adjustment factors to accommodate some of the peculiarities of worm gears. Values for the modification factors were deduced or evaluated and their combined influence gives about 34% reduction in the bending stress of worm gears when compared to cylindrical helical gears of the same size and under similar loading. The study shows that the enhance bending capacity of worm gears is largely due to throating.

The root bending stress computations of five wormset designs from different references were carried out using the current model. In Table 5, the variances between the current and the previous stress estimates in the references are in the range of -32.3 and –3.8% for exactly the same design parameters. This shows that the previous solutions appear to be conservative when compared to the results of the new root bending stress capacity model. However, when the service load factor is evaluated using Eq. (10) or Eq. (A1) as suggested in Appendix A, the variances between the current and the previous root bending stress estimates are in the range of -13.3 and 2.4%. These variances seem to indicate very good correlations with the previous estimates. Consequently, it seems that a more reliable analytical method for estimating the root bending stress of cylindrical worm drives has been formulated.

12.0 ACKNOWLEDGEMENTS

The authors gratefully acknowledge that this study was supported in parts with funds from College of Science, Engineering, and Technology (COSET) Research Fund and the University Faculty Development Fund of Texas Southern University, Houston, Texas.

13.0 NOMENCLATURE

1 - subscript for worm
2 - subscript for gear
a_1 – AGMA velocity exponent
a_2 – AGMA velocity coefficient
b – gear facewidth (mm)
b_1 – active threaded length of worm (mm)
b_2 – active facewidth of gear
b_g – nominal facewidth of gear
b_w – nominal facewidth of worm (mm)
c_f – root clearance factor
d – gear pitch diameter (mm)
d_a – addendum diameter (mm)
E – elastic modulus of pinion or gear material (GPa)
E_c – composite or effective elastic modulus (GPa)
F_a – axial force (N)
F_n – normal contact force (N)
F_r – radial force (N)
F_t – tangential force (N)
H_s – Surface hardness: Vicker's number
k_c – friction load coefficient
k_t – stress combination factor
k_m – mesh friction gear material factor
k_σ – normal stress concentration factor
k_τ – shear stress concentration factor
K_a – load application factor
K_A – adjusted load application factor
K_f – mesh frictional load factor
K_m – mesh overload factor
K_o – spur gear internal overload factor
K_s – service load factor
K_v – internal dynamic overload factor
K_w – worm thread load factor
l_m – moment arm (mm)
$l_m^{/}$ – apparent moment arm (mm)
m_a – axial module (mm)
m_n – normal module (mm)
m_t – transverse module (mm)
n_g – number of gear teeth on effective threaded length of worm
n_t – minimum apparent design factor for bending resistance
n_b – apparent design factor for bending resistance
N_1 – rotational speed of worm (rpm)
N_2 – rotational speed of gear (rpm)
p_a – axial pitch (mm)
P_1 – transmitted power by worm (kW)
q_n – gear profile quality number
$r_2^{/}$ – apparent pitch radius of worm gear (mm)
r_2 – pitch radius of worm gear (mm)
r_f – gear root fillet radius (mm)
r_t – gear throat radius (mm)
S_{yt} – tensile yield strength (MPa)
S_t – allowable root bending stress (MPa)
S_f – service fatigue strength (MPa)
S_{ut} – tensile strength (MPa)
t_a – actual circular tooth thickness (mm)

t_b – tooth backlash (mm)

t_r – gear root thickness (mm)

T – torque transmitted by a gear (Nm)

T_1 torque transmitted by worm (Nm)

T_2 – torque transmitted by gear (Nm)

u – speed ratio

V_s – sliding velocity (m/s)

V_t – tangential velocity at pitch point (m/s)

x_n – normal profile-shift factor

y – apparent pitch radius increases (mm)

Y_b – Lewis stress factor

Y_f – effective fatigue strength factor

Y_n – bending fatigue durability factor

Y_s – surface finish factor (steel only)

Y_x – size factor

Y_r – gear reliability factor

Y_i – directional bending stress factor

z_1 – number of threads on worm

z_2 – number of gear teeth

z_v – number of virtual teeth

z_{v2} – number of gear virtual teeth

z_w – worm form number

α_e – contact effectiveness factor

β_f – nominal pulsating fatigue ratio at 99% reliability

β_o – effective strength increase factor

β_1 – gear throating strengthening factor

β_2 – worm arc load strengthening factor

β_3 – gear apparent profile-shift strengthening factor

β_4 – gear tooth thickness strengthening factor

θ_1 – worm face half-angle (deg.)

θ_2 – gear face half-angle (deg.)

κ – gear root thickness factor

κ_1 – approach length factor

κ_2 – recess length factor

σ_t – root bending stress (MPa)

ϕ_a – addendum contact angle (deg.)

ϕ_n – normal pressure angle (deg.)

ϕ_t – transverse pressure angle (deg.)

ϑ_m – mesh friction coefficient

λ_a – moment arm factor (mm)

λ_r – rim backup ratio

η_w – worm efficiency

γ – worm lead angle (deg.)

γ_o – optimum worm lead angle (deg.)

ϖ_v – virtual contact ratio

ϖ_c – theoretical contact ratio

ϖ_s – load sharing factor

λ_c – worm contact coefficient

ψ – nominal helix angle of gear (deg.)

ψ_b – base helix angle of gear (deg.)

η_w – wormset efficiency

χ_a – axial force factor

α_b – backlash decimal fraction

χ_b – backlash tooth thickness factor

14.0 REFERENCES

[1] Rexnord, Failure Analysis-Shafts-Bearings-Seals, Rexnord Industries, August, pp. 1 – 13, 1978.

[2] Berezovlsky, Y., Chernilevsky, D., Petrov, M., Machine Design, MIR, Moscow, 1988.

[3] Orthwein, W., Machine Component Design, West Publishing Company, New York, 1990.

[4] Leidich, E., and Reissmann, J., Calculations of the Tooth Root Strength of Worm Wheel Teeth Based on Local Stresses, Gear technology, Nov./Dec., 2016.

[5] Dobrovolsky, Zablonsky, K., Mak, S., Radchik, A., and Erlikh, L. Machine Elements, Foreign Language Publishing House, Moscow, 1965, pp. 33 – 34; 279 - 289.

[6] Maitra, G. M., Fundamentals of Toothed Gearing: Handbook of Gear Design, 2nd ed., McGraw Hill, Delhi, 2013.

[7] Octrue, M., Evolution of Worm Gear Standards and their Consequences on Load Capacity Calculations, Power Transmission Engineering, 2014, 36 – 42.

[8] Mostafa, M. A., Mechanics of Machinery, CRC Press, New York, 2013.

[9] Budynas, R. G. & Nissbett, J. K., Shigley's Mechanical Engineering Design, 9th Edition, McGraw Hill Education, 2010.

[10] Jang, W., Analysis and Design of Machine Elements, Wiley, Singapore, 2019.

[11] Dudley, D. W., Handbook of Practical Gear Design, CRC Press, 2004.

[12] Kapelevich, A., Direct Gear Design, CRC Press, New York, 2013.

[13] Edward E. Osakue and Anetor, L., Revised Lewis Bending Stress Capacity Model for Cylindrical Gears, The Open Mechanical Engineering Journal, Vol. 14, pp. 3 – 16, 2020.

[14] Gope, P. C., Machine Design: Fundamentals and Applications, PHI Learning, Delhi, 2014.

[15] Osakue, E. E. and Anetor, L., Contact Stress Capacity Model for Cylindrical Worm Gears, FME Transactions, 50, 1-15, doi: 10.5937/fme2201001O, 2022.

[16] Osakue, Anetor, L. and Harris, K., A Parametric Study of Frictional Load Influence in Spur Gear Bending Resistance, FME Transactions journal, 48, 294 – 306, 2020.

[17] AGMA documents AGMA 2001-D04, Fundamental Rating Factors and Calculation Methods for Involute Spur and Helical Gear Teeth: http://wp.kntu.ac.ir/asgari/AGMA%202001-D04.pdf

[18] Hamrock, p. 396, p. 430; Schmid, S. R., Hamrock, B. J. & Jacobson, B. O., Fundamentals of Machine Elements, 3rd ed., CRC Press, New York, 2014.

[19] Khurmi, R. S. and Gupta, J. K., A Textbook of Machine Design, Eurasia Publishing House, New Delhi, 1980,
Osakue, E. E. and Anetor, L., Helical Gear Bending Fatigue Design, Int'l Journal of Research in Engineering and Technology, 2017, Vol. 06, Issue 04, 2017.

[20] Osakue, E. E., Extending Revised Lewis Gear Root Bending Stress Model to Addendum Modified Cylindrical Gears, International Research Journal of Engineering and Technology, Vol. 12, Iss. 07, pp. 254 - 271, 2025.

[21] Osakue, E. E., and Saneifard, R., A Bevel Gear Root Bending Stress, International Research Journal of Engineering and Technology, Vol. 12, Iss. 09, pp. 325-343, 2025.

[22] ISO 6336-3:2006-09,Calculation of Load Capacity of Spur and Helical Gears -- Part 3: Calculation of Tooth Bending Strength.

[23] KHK,TechnicalReference,https://khkgears.net/new/gear_ knowledge/gear_technical_reference/bending-strength-of-spur-and-helical-gears.html.

[24] SDP/SI] SDP/SI, Elements of Metric Gear Technology, https://www.sdp-si.com/resources/elements-of-metric-gear-technology.

[25] DET NORSKE VERITAS, (2003), Calculation of Gear Rating for Marine Transmissions, Classification Notes, No. https://rules.dnvgl.com/docs/pdf/DNV/cn/201205/CN41-2.pdf.

[26] Skakoon, J. G., Detail Mechanical Design: A Practical Guide, ASME Press, New York, p. 144, 2000.

[27] Chernilevsky, D., A Practical Course in Machine Design, MIR, Moscow, p. 93, 1990.

[28] Osakue, E. E. and Anetor, L., Design Sizing of Cylindrical Worm Gearsets, FME Transactions, Vol. 48, No 1, pp. 31 - 45, doi:10.5937/fmet2001031O, 2020.

[29] Mott, R. L., Machine Elements in Mechanical Design, 4th Ed., Prentice Hall, New York, 2004.

[30] WormGears,https://khkgears.net/new/worm_gear.html.

[31] Childs, P. R. N., Mechanical Design Engineering Handbook, Butterworth-Heinemann, Elsevier, New York, 2014.

[32] Rortbart, H. A. & Brown, T. H., Mechanical Design Handbook, 2nd ed., McGraw-Hill, New York, 2006.

[33] Crosher, W., ToothTips, Gear Solutions, p. 23,Jan.,2012,https://gearsolutions.com/media/uploads/uploads/assets/PDF/Articles/Jan_12/0112_ToothTips.pdf.

[35] Dengel, B., Eliminating Backlash in Worm Gears Pairs, Gear Solution, May 15, 2022.

[36] Andrzel Maciejczyl and Zbigniew Zdziennicki, Design Basicsof Industrial Gear Boxes,

https://cybra.lodz.pl/Content/3714/DesignBasicInd.pdf.

[37] KISSsoft Tutorial 16, Analyzing the Geometry of Cylindrical Worm Gears with Enveloping Worm Wheel;https://old.kisssoft.ag/english/downloads/pdf/03-17/kisssoft-tut-016-E-wormgear.pdf.

[38] MITCal, Worm Gear Geometric Design and Strength Check,https://www.mitcalc.com/en/ui/wormgear.pdf

[39] Chernilevsky, D., Lavrova, E., and Romanov, V. Mechanics for Engineers, MIR Publishers, Moscow, 1984.

[40] Conrado, E. and Davoli, P., The True Bending Stress in Spur Gears, geartechnology.com, August 2007.

[41] Shaoshuai Hou, Jing Wei, Aiqiang Zhang, Teik C. Lim, Chunpeng Zhang, Study of Dynamic Model of Helical/Herringbone Planetary Gear System with Friction Excitation, J. Comput. Nonlinear Dynam. 13(12): 121007, 2018; https://doi.org/10.1115/1.4041774.

[42] Walsh, R. A., Electromechanical Design Handbook, 3rd ed. McGraw Hill, New York, 2000, p. 8.78.

[43] Juvinall, R. C. and Marshek, K. M. Juvinall's Fundamentals of Machine Component Design, S.I. Version, Wiley, Singapore, p. 551, 2017.RoyMech: GearsGearEfficiency,www.roymech.co.uk/Useful_Tables/Drive/Gear_Efficiency.html, 2018.

[45] Bhadari, V. B., Design of Machine Elements, McGraw-Hill (India), New Delhi, 2010.

[46] Hannah, J. , and Stephens, R. C., Mechanics of Machines: Advanced Theory and Examples, Edward Arnold, London, 1972.

APPENDIX A: WORM GEAR SERVICE LOAD FACTOR

The design or expected service load is often estimated by multiplying the rated load with a service load factor having a value greater than unity. It takes care of load excitations beyond the rated value that are reoccurring in normal operations of gearsets. It does not account for peak or momentary overload. The service load factor has several components such as the load application factor, internal dynamic overload factor, mesh overload factor, tooth rigidity factor, etc. For wormsets, it may be evaluated from Eq. (10) or Eq. (A1).

$$K_s = K_a K_v K_m K_f K_w \quad \text{(A1)}$$

A1: Load Application Factor (K_a)

The load application factor accounts for load increases caused by the power source device and the driven or load device on gear drives. It is indicative of the influences of the accelerations and decelerations of external masses connected to the gear drive. The values for wormsets are slightly lower than those of other gear types due largely to the fact that worm gearsets are quieter when running. Values of K_a are established from experience over a considerable time period in an industry based on "good" practice in design, manufacturing, installation, and operations. Companies may generate their own data, however organizations such as AGMA, ISO, JIS, etc provide recommendations. It is generally between 1.0 and 2.0 for wormsets, where 1.0 is applicable to uniform load situations, and 2.0 is applicable to heavy shock situations [24].

A2: Internal Overload Factor (K_v)

The noise and vibrations generated during gearset operations are indicative of the level of additional internal load that is created in geared systems due to local dynamics of moving parts. The internal overload factor accounts for these internal load excitations which are caused by manufacturing inaccuracies. The noise and vibrations are caused by non-conjugate actions of meshing gear teeth, accelerations and decelerations of internal moving parts, dynamic imbalance of internal parts, and the additional excitations caused by backlash, profile errors, pitch errors, etc. In wormsets, the operation is generally smooth and quiet as the worm threads continuously slide on the gear teeth [14]. However, the internal vibrations and noise can be made worse by the sliding action in the mesh due to frictional resistance [41]. Hence, the sliding velocity is critical in determining the internally generated overload in wormsets. In ANSI/AGMA standards for cylindrical [17], the value of K_v is based on the gear pitch velocity and the gear profile manufacturing quality number. The standard has twelve quality grade numbers of 1 to 12, with lower numbers representing higher qualities. The two intermediate parameters for estimating the internal dynamic overload factor based on AGMA [17] recommendations are expressed in Eq. (A2).

For $6 \le q_n \le 12$:

$$a_1 = 0.25(q_n - 5)^{2/3} \quad a_2 = 3.5624 + 4(1 - a_1) \qquad \text{(A2)}$$

The sliding velocity in wormsets is obtained from Eq. (A3).

$$V_s = \frac{\pi d_1 N_1}{60 \cos\gamma} \times 10^{-3} \qquad \text{(A3)}$$

Eq (A4a) gives the expression for estimating the internal overload factor for finished machined metallic spur gears. Eq (A4b) is suggested for the internal overload factor of a worm gear when considered as a cylindrical helical gear.

$$K_o = \left[1 + \frac{\sqrt{V_s}}{a_2}\right]^{a_1} \qquad K_v = 1 + 075(K_o - 1) \qquad \text{(A4)}$$

$$K_m \approx 1.025 + 0.93\frac{b_2}{d_2}\left[0.2 + 0.0112\left(\frac{K_A d_2 T_2}{b_2}\right)^{1/3}\right] \qquad \text{(A5a)}$$

$$K_A = K_a K_v^2 K_f K_w \qquad \text{(A5b)}$$

The internal dynamic load is to some extent dependent on the nominal helix angle in helical gears because it has the effect of producing gradual teeth engagement in a mesh, which reduces the internal dynamic overload. Therefore, the dynamic load of a helical gear may be taken to be about 75% of that a spur gear [6, p. 2.90] as given in Eq. (A4b) for machined metallic helical gears.

Wormsets are the smoothest and quietest forms of gear drives [42], indicating that the internally generated excitations are relatively low compared to other types of gear drives. This is partly due to the continuous sliding of thread(s) on gear teeth without break in contact during operation. It is suggested that the value of K_o should be at most 1.25 when selecting worm gear manufacturing profile grade. The worm profile grade is usually one grade better than that of the worm gear. For general application, worms are made to profile accuracy grades 8 to 6 [10].

A3: Worm Gear Mesh Overload Factor (K_m)

The mesh overload factor accounts for the non-uniform spread of the transmitted load across meshing gear facewidths due to misalignment of the gears. The misalignment is caused by dynamic twisting and bending of gears and supporting members due to the transmitted forces. The misalignment depends primarily on the lateral rigidity of shafts, and secondarily on the rigidity of gears and housing members. Generally, precise value for the mesh overload factor is difficult to estimate for gear drives.

The lateral rigidity of cylindrical wormsets is comparable to that of cylindrical gears and that of globoidal wormsets is about the same as that of bevel gear drives in design practice [2]. Hamrock et al [18, p. 409] provided an expression for a rough approximation of K_m for cylindrical gears as a function of pinion torque, pinion facewidth, pinion pitch diameter, and the load application factor. That expression is here adapted for cylindrical wormsets with some modifications as given in Eq. (A5a), where the parameters of the worm gear are used instead of those of the worm. The other modifications include the use of an adjusted load factor (Eq. (A5b), the use of constant 1.025 instead of 1.0 for a more conservative estimate, and the inclusion of the 0.93 coefficient.

The adjusted load factor of Eq. (A5b) is used instead of the load application factor to better approximate the load on the gear and also to avoid an iterative evaluation of the service load factor and mesh overload factor, since K_m is a component in Eq. (A1) for K_s. K_A is an approximation of K_s which is usually higher than K_a. The helix angle has the effect of slightly reducing the transmission error in helical gearsets, making them slightly less sensitive to assembly and manufacturing errors. This may reduce the mesh overload factor of spur gears to about 93% for helical gears [43]. For this reason, the coefficient 0.93 is applied to the incremental portion in Eq. (A5a).

A4: Frictional Load Factor, (K_f)

The frictional load factor accounts for the additional load experienced in gear meshes due to the presence of friction. Gear mesh friction is complicated with contributions from sliding and rolling motions. In worm drives, sliding friction in the mesh is predominant. An average wormset mesh friction model based on sliding motion and modified by a material type factor may be estimated from Eq. (6a) and Eq. (A6b). The expressions are based on good lubrication of a casehardened steel worm mating with a phosphor bronze gear. Eq. (6a) is used for low sliding velocities, where $0 < V_s \le 3$ m/s :

$$\vartheta_m = \left(0.043 - 0.0151\mathrm{Log_e}(V_s)\right) k_m \qquad \text{(A6a)}$$

Eq. (6b) is used for higher sliding velocities, where $V_s > 3$ m/s :

$$\vartheta_m = \frac{0.031 k_m}{V_s^{1/4}} \qquad \text{(A6b)}$$

The parameter k_m depends on the worm gear material and is 1.0 for phosphor bronze, 1.15 for aluminum bronze, and 1.20 for cast iron [44]. For thru-hardened worms, the value from Eq. (A6) may be multiplied by 1.25. If the worm is unground, 30% to 50% increase in friction value is not unlikely [6, 9]. Worms and worm gears are usually made of dissimilar materials to minimize the frictional resistance and improve conformability of the worm gear teeth surfaces with the thread profile of the worm [45]. Frictional resistance is lower for smooth surfaces, therefore, after they have been cut and heat-treated, worms are usually ground and sometimes polished [2].

The frictional load factor for worm drives is assumed to consist of gear mesh and screw frictional load components [15, 29] and may be obtained from Eq. (A7).

$$K_f = (1.0 + \vartheta_m)\left[1 - \frac{\vartheta_m \tan\psi}{\cos\phi_n}\right]^{-1} \qquad \text{(A7)}$$

A5: Worm Thread Profile Load Factor, (K_w)

Different types of profiles may be used for the worm thread and the common thread profiles are designated as ZA, ZN, ZK, ZI, and ZC [6]. The influence of the worm profile type on the load capacity of a wormset is captured by the worm thread profile factor given in Table A1.

APPENDIX B: LEWIS STRESS FACTOR

Eq. (12a) incorporates the parameter Y_b , a modified version of the famous Lewis form factor and defined as the Lewis stress factor in this study. Y_b is similar to the reciprocal of the AGMA J-factor but is independent of the stress concentration factor and load sharing. It is based on a gear root fillet radius of $0.375m_n$, gear tooth whole height of $2.25m_n$, and standard pressure angle of 20^o. Y_b is a function of the virtual number of teeth on a gear and the profile- shift factor as expressed in Eq. (13). The virtual number of teeth for a helical gear is obtained from Eq. (2b). Fig. B1 shows a plot of Y_b against the virtual number of teeth on a cylindrical gear, for different values of profile-shift factors in the range -0.5 to 1.0. The values of Y_b for profiled-shifted and standard profile gears can be obtained from Fig. B1.

Table A1: Worm Thread Profile Factor (K_w)*

ZA/ZN	ZI/ZK	ZC
1.00	0.80	0.60

*From ref. [29]

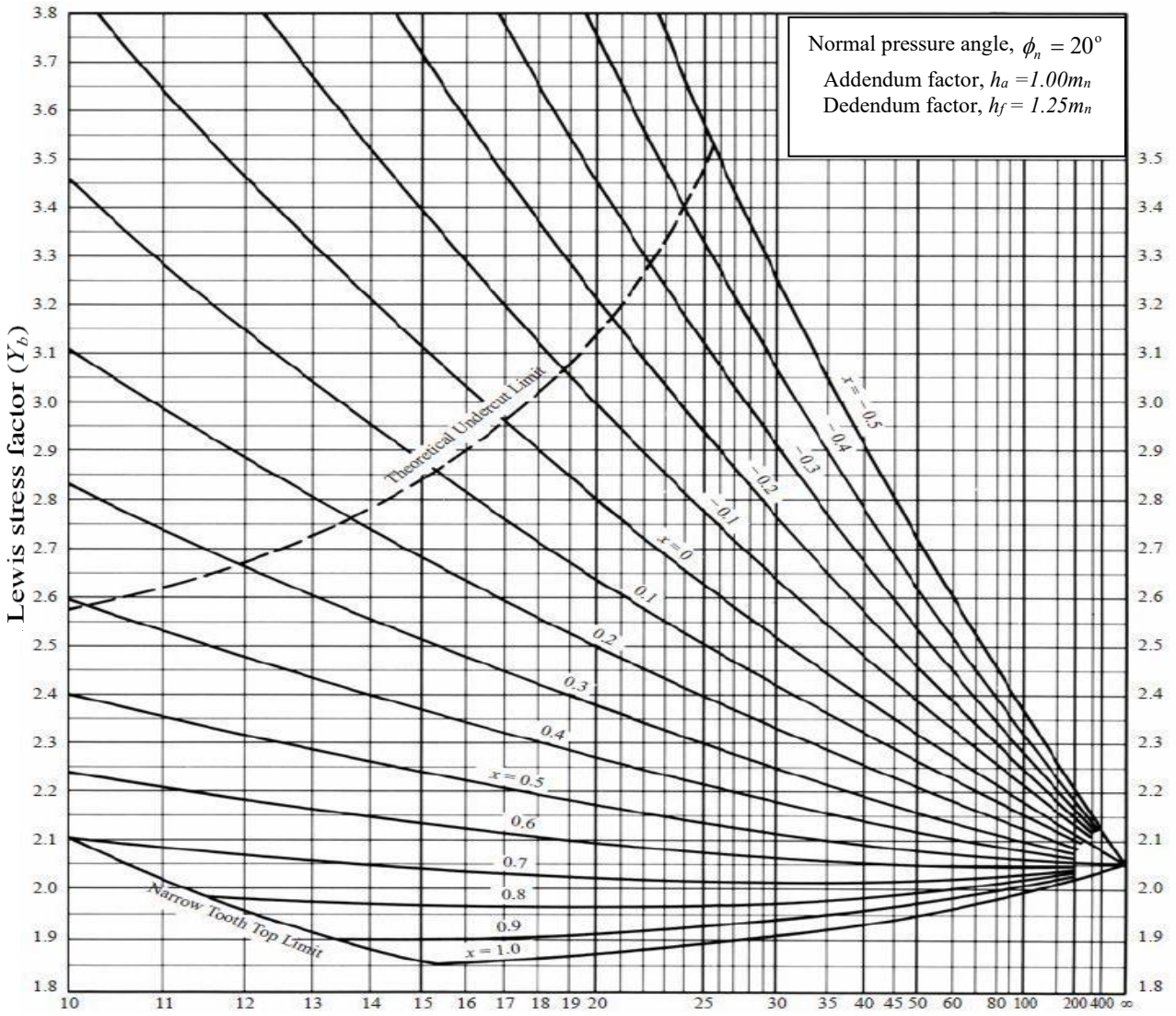

Virtual gear teeth number (z)

Fig. B1: Lewis stress factor (24, 25)